Materials Science Forum
ISSN: 1662-9752, Vol. 1190, pp 55-62
doi:10.4028/p-Jc6le5
© 2026 The Author(s). Published by Trans Tech Publications Ltd, Switzerland.
Submitted: 2025-09-27
Revised: 2026-01-21
Accepted: 2026-01-31
Online: 2026-05-18

Investigation of Spoke Pattern of Stacking Faults in 4H-SiC Wafers Grown by Physical Vapor Transport Method

Zeyu Chen[1, a *], Jianpei Zhang[1,b], Shanshan Hu[1,c], Kaixuan Zhang[1,d], Yuzhuo Li[1,e], Haochi Wang[1,f], Balaji Raghothamachar[1,g], Yafei Liu[2,h], Campbell Bouch[2,i], Ryan Philpott[2,j], Scott Turchetti[2,k], Pete Schunemann[2,l] and Michael Dudley[1,m]

[1]Department of Materials Science & Chemical Engineering, Stony Brook University, Stony Brook, NY, 11794, USA

[2]Onsemi, 55 Executive Drive, Hudson, NH, 03051, USA

[a]zeyu.chen@stonybrook.edu, [b]jianpei.zhang@stonybrook.edu, [c]shanshan.hu@stonybrook.edu, [d]kaixuan.zhang@stonybrook.edu, [e]yuzhuo.li@stonybrook.edu, [f]haochi.wang@stonybrook.edu, [g]balaji.raghothamachar@stonybrook.edu, [h]yafei.liu@onsemi.com, [i]Campbell.Bouch@onsemi.com, [j]Ryan.Philpott@onsemi.com, [k]Scott.Turchetti@onsemi.com, [l]Pete.Schunemann@onsemi.com, [m]michael.dudley@stonybrook.edu

Keywords: 4H-SiC; Characterization; X-ray Topography; Defects

Abstract. Synchrotron monochromatic beam X-ray topography (SMBXT), synchrotron white beam X-ray topography (SWBXT) and high-resolution X-ray topography (HRXRT) were used to characterize a series of wafers sliced from two PVT-grown 4H-SiC boules under similar growth conditions. A unique spoke-shaped distribution of the threading screw/mixed dislocations (TSDs/TMDs) density map can be observed from wafers sliced from later stages of growth of both boules. Systematic sequential analysis of the SMBXT grazing incidence images and HRXRT reflection images of the wafers reveals the spoke patterns are formed due to continuous deflection process of TSDs/TMDs by thin layer of polytypes that propagate along step flow direction and expand vertically, leading to TSD density difference across the wafer. Regions with high TSD densities have higher growth rate, resulting in a ridge and valley structure. Generation of macrosteps in the valley regions due to regular step structure deflect more TSDs/TMDs that then form mixed type (Shockley+Frank) stacking faults.

Introduction

Silicon carbide (SiC) is a semiconductor with a wide bandgap and exceptional electronic and physical properties, including high saturation velocity, high breakdown field, and excellent thermal conductivity [1]. These attributes make SiC a highly promising material for demanding applications involving high voltage, high power, and high temperature environments. The development of large-scale, high-quality single crystal SiC substrate wafers is crucial for enhancing device performance and broadening its application scope. Among the available growth techniques, physical vapor transport (PVT) [2] is the most widely used method, as it allows the production of large SiC substrates with controllable growth rates. However, the presence of various crystallographic defects, such as threading screw/mixed dislocations (TSDs/TMDs) and micropipes (MPs) can significantly impact device performance, limiting the full potential of SiC-based technologies [3,4]. Therefore, the generation and impact of such defects during PVT growth should be thoroughly investigated to improve the growth process and furnace design.

Besides replication from the seed, TSDs/TMDs pairs are usually generated at the seed interface if large stress is present or at the interface of inclusions [5-7]. Deflections of TSDs/TMDs onto the basal plane have been observed previously [8], where TSDs/TMDs get deflected by macrosteps formed at the later stage of the growth when the curvature of the growth interface becomes higher. In this study, series of 4H-SiC wafers sliced from two boules grown under similar conditions were analyzed by synchrotron white beam X-ray topography (SWBXT) in 1-100 and 1-101 reflections to map the

This article is an open access article under the terms and conditions of the Creative Commons Attribution (CC BY) license
(https://creativecommons.org/licenses/by/4.0)

distribution of stacking faults. Mappings of TSDs/TMDs densities were conducted by high resolution X-ray topography (HRXRT) in 0008 reflection, where relatively high density of TSDs/TMDs are nucleated at the beginning of the growth, that then continuously get deflected as the growth proceeds. Such deflected TSDs/TMDs can possibly dissociate into partials dislocations bounding Frank type/mixed (Frank+Shockley) type stacking faults [9,10], which will lead to increase of forward voltage and leakage currents [11-14]. The nature and mechanism of such deflection process need to be analyzed carefully in order to improve the design of the furnace and refine the growth processing.

Experiment

Series of wafers sliced from two PVT-grown boules have been characterized and the position of the wafers with respect to the boules are shown in Fig. 1. Synchrotron Monochromatic Beam X-ray Topography (SMBXT) in grazing incidence geometry is an X-ray imaging technique capable of revealing the structural defects in the crystal up to a depth of 17µm. Monochromatic beam (E = 8.9 KeV) is used in SMBXT and 11-28 grazing incident reflection is recorded on high resolution X-ray films. Synchrotron white beam X-ray topography (SWBXT) in transmission geometry are used to characterize stacking faults and 1-100 and 1-101 reflection via SWBXT were recorded. Experiments were carried out at Beamline 1-BM at the Advanced Photon Source (APS), Argonne National Laboratory. Ray-tracing simulation was conducted for inclusion contrast on topographs of 4H-SiC in 11-28 reflection through a Python algorithm based on orientation contrast model [15].

High-resolution x-ray topography (HRXRT) was performed using a Rigaku XRTMicron system. XRT image of TSDs/TMDs was acquired using g = [0008] in reflection geometry with CuKα radiation. TSD maps were generated by XRT Toolbox software, an automatic XRT data processing tool to generate defect analysis reports.

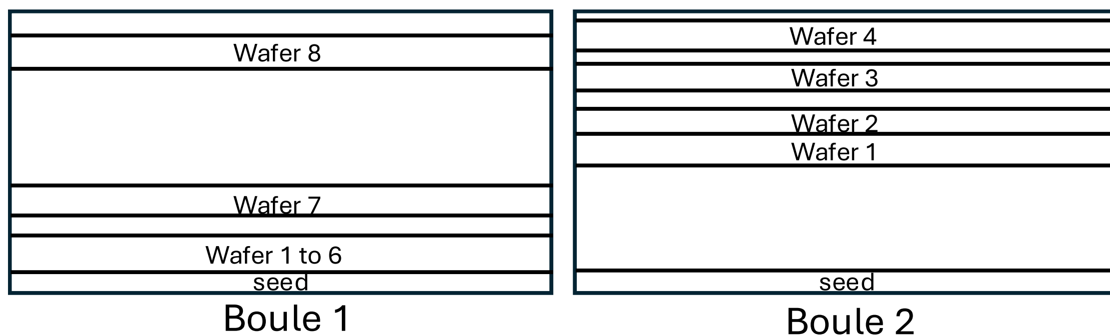

Fig. 1. Schematic diagram of PVT boules showing position of wafers sliced from the boules discussed in this study.

Results and Discussion

Selected areas of HRXRT images in 0008 reflection of wafer1, 2, 4 and 5 of boule 1 are shown in Fig. 2(a), 2(b), 2(d), 2(e), 2(g) and 2(h), respectively with wafer1 closest to seed. Some of the line features observed on the topographs are highlighted by dashed red lines in images of wafer1 and wafer4, as shown in Fig. 2(a), 2(d) and 2(g). These features are observed to propagate and expand during growth as highlighted with orange dotted lines in images of wafer2 and wafer5, as shown in Fig. 2(b), 2(e) and 2(h). The stacked images, as shown in Fig. 2(c), 2(f) and 2(i), indicate that the line features propagate along the radial step flow direction and expand along [1-100] or [-1100] directions. To further investigate, SMBXTs in 11-28 reflection of wafer4 and wafer5 are shown in Fig. 3(a) and 3(b), where the line features are indicated by the red dotted line. Similar to the observation from HRXRT, the same line features can be detected from SMBXTs of wafer4 and wafer5, indicating that the line feature propagated in the boule on the basal plane during growth and deflected a bundle of TSDs/TMDs as indicated by the orange arrows. Ray tracing simulation was conducted to show contrast of a column of inclusion, where the result, as shown in Fig. 3(c), indicates white line contrast bounded by two dark lines, correlating with the line contrast observed from SMBXTs. Since the line

features have same contrast as a column of inclusions and they can propagate and expand on the basal plane, it strongly indicates that the line features are likely polytypes. Besides, since the width of the line feature in SMBXTs is around 40μm comparable to the width of deflected TSDs/TMDs, the actual thickness of the polytype layers can be extremely small (tens of Å).

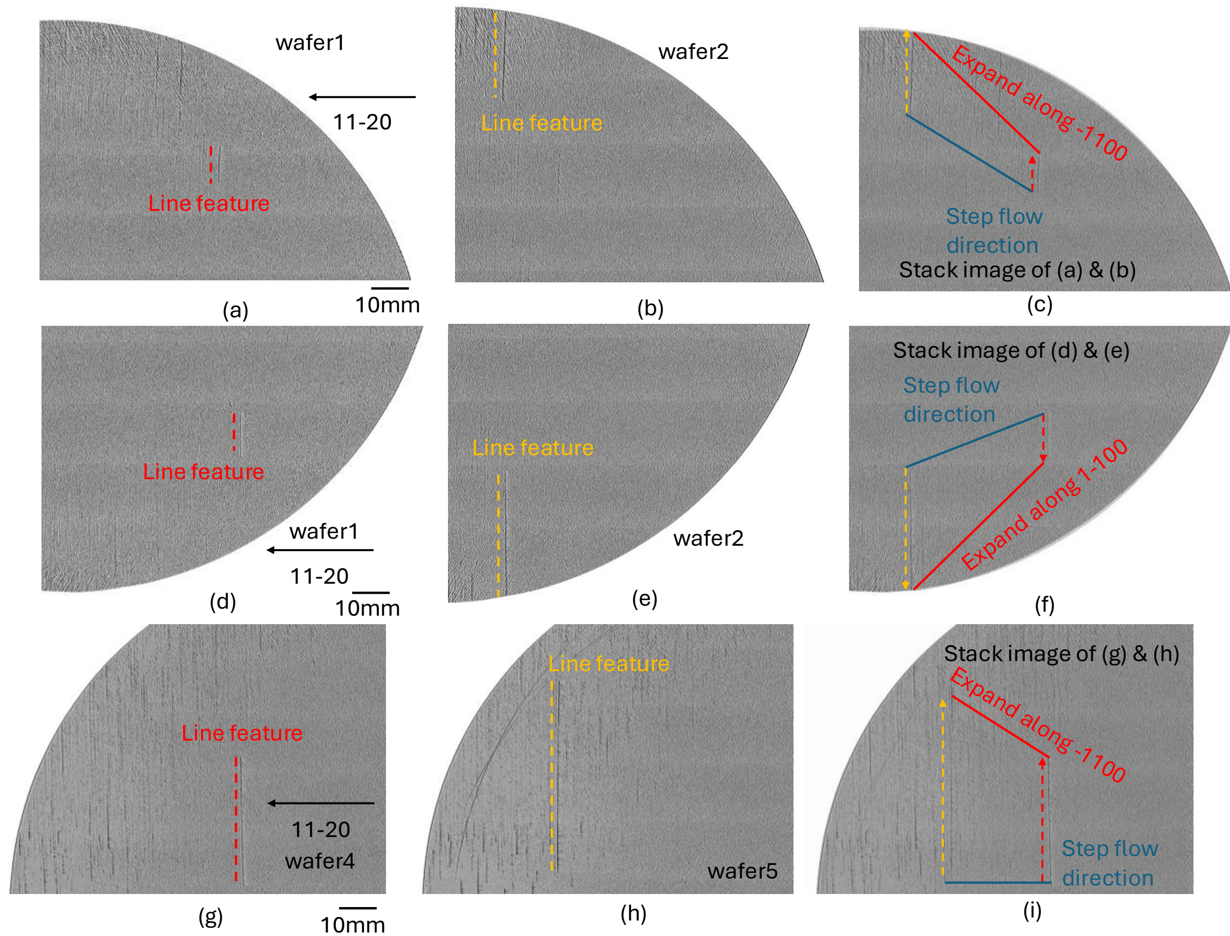

Fig. 2. HRXRT images of (a) and (d) wafer 1 of boule 1; (b) and (e) wafer 2 of boule 1; (g) wafer 4 of boule 1 and (h) wafer 5 of boule 1. (c), (f) and (i) show stacked images of (a) and (b), (d) and (e), (g) and (h) respectively. Line features can be observed in individual images, and the stacked images indicate such line features propagate along step flow direction and expand along [1-100] or [-1100] direction.

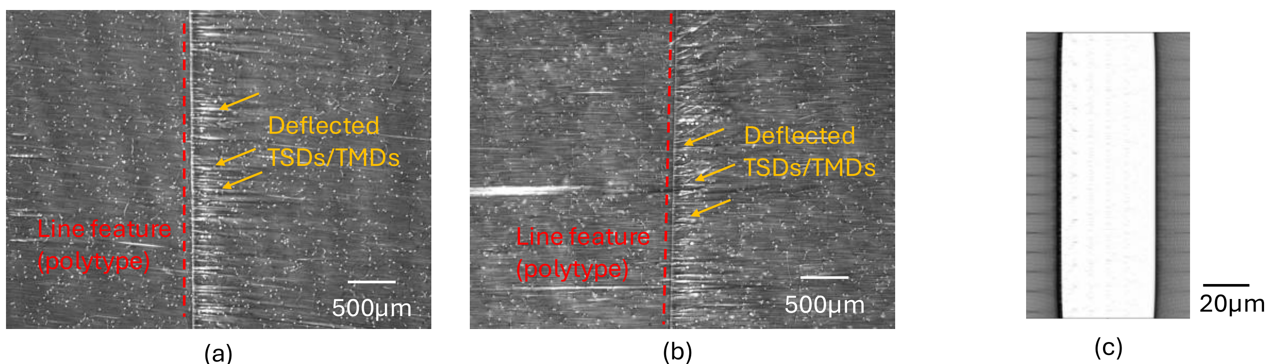

Fig. 3. 11-28 SMBXT of (a) wafer 4 and (b) wafer 5, showing that the line features deflect TSDs/TMDs. (c) shows ray tracing simulation of a column of inclusions.

Deflection of TSDs/TMDs by polytype can be observed in Fig. 3(a) and 3(b). Fig. 4(a) depicts 3D schematic of nucleation of polytype, where 2D nucleation takes place on the flat terrace due to relatively fast growth, then the polytype will then expand with the step as shown in Fig. 4(b) and 4(c). The polytypes will deflect TSDs/TMDs, since the Burgers vectors of TSDs/TMDs in 4H are not

compatible with the polytype, and deflection onto the basal plane will be more energetically favorable. In addition, misfit stress between the polytype and the newly grown layer will also facilitate nucleation of new TSDs/TMDs as shown in Fig. 4(d).

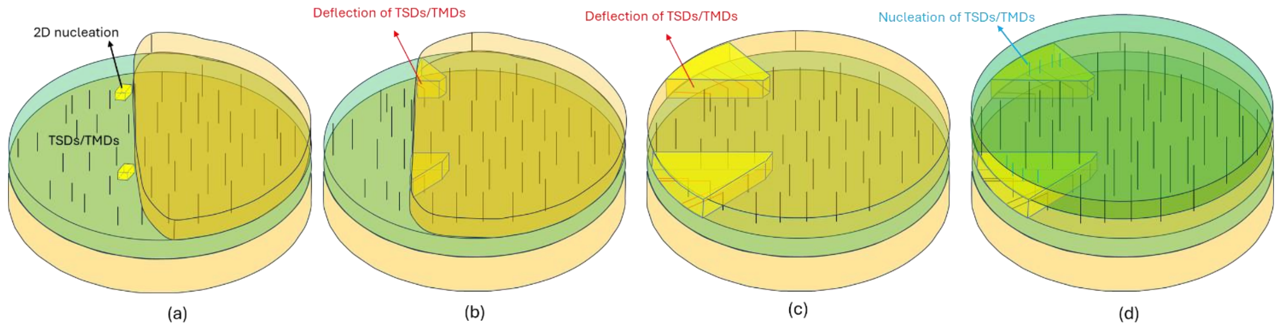

Fig. 4. Schematic of (a) nucleation of polytype, (b) and (c) deflection of TSDs/TMDs by polytype and (d) nucleation of TSDs/TMDs from polytype.

Fig. 5 shows the propagation and expansion of polytype at different parts of the wafer and with vertical step and curved step directions. At the beginning of the growth the step direction will be vertical near the central part of the wafer then slightly curved around the edge since the relatively flat growth front, as shown by T. Ailihumaer and coworkers [16]. Fig. 5(a) and 5(b) show propagation and expansion process of wafer 1 of boule 1 (stack image shown in Fig. 2(c) and 2(f)), and Fig. 5(c) and 5(d) show the process of wafer 4 of boule 1(stack image shown in Fig. 2(i)). As discussed above, the inner edge of the polytype will follow the step flow direction (perpendicular to step direction) and the other edge will expand along vertically, where faster growth takes place toward the edge of the wafer since C/Si ratio is higher at the position closer to the graphite crucible. Moreover, the polytypes expand quickly and occupy relatively large area of the wafer since the vertical step direction along [1-100] or [-1100] is the shortest distance to the edge of the wafer. Fig. 5(i) and 5(j) show comparison between polytype in wafer3 at early stage of growth and wafer7 at later stage of growth, where the size of the polytypes are slightly smaller in wafer7. When the growth proceeds to the later stage, the step direction will become curved as the curvature of the growth interface increases. Under such circumstances, the step direction will no longer be the shortest distance to the edge of the wafer, so the expansion will take place slightly slower, as indicated in Fig. 5(e) and 5(f). If the polytype is generated at the center of the wafer, both edges of the polytype will expand, since the gradient of C/Si ratio are similar for both sides.

Fig. 6(a) to 6(d) indicates TSDs/TMDs density map of wafer3, wafer6, wafer7 and wafer8, where red color means that TSDs/TMDs density is higher than manually set threshold value. Since deflections of TSDS/TMDs have been observed in HRXRT, the decrease of TSDs/TMDs density can be mainly attributed to deflections of TSDs/TMDs by the polytype layers. Even though deflection by polytype layers take place continuously starting from wafer1, such polytypes also nucleate new TSDs/TMDs as explained previously, so TSDs/TMDs density is relatively high at the early growth stage, as shown in Fig. 6(a). It should be noted that the remaining TSDs/TMDs formed a spoke-like pattern at the later stage of growth (Fig. 6(b) to 6(d). As the growth proceeds to wafer 6, the step direction becomes curved and the expansions of polytypes are slower. Fig. 6(e) depicts propagation and expansions of multiple polytypes, where one side of the polytypes at the inner region follow the step flow direction (dashed line) and the other side will expand (solid line), and polytype at the center will expand on both sides. It can be observed that the gaps between the polytypes, formed due to the difference between propagation and expansion direction, correlate with the spoke-like feature in Fig. 6(d), since fewer deflections will take place in the gap region.

Deflection process starts from the left side first (Fig. 6(b) and 6(c)) and the deflection on the right side of the wafer takes place at the later stage (Fig. 6(d)). As shown in Fig. 6(f), when the interface is slightly curved, the width of the terrace is longer on the left side, then as the curvature of the growth interface increase, the facet will migrate towards the center of the boule, shortening the terrace on the left side and terrace on the right side will become longer, where a longer width of the terrace will increase the probability of 2D nucleation of polytype.

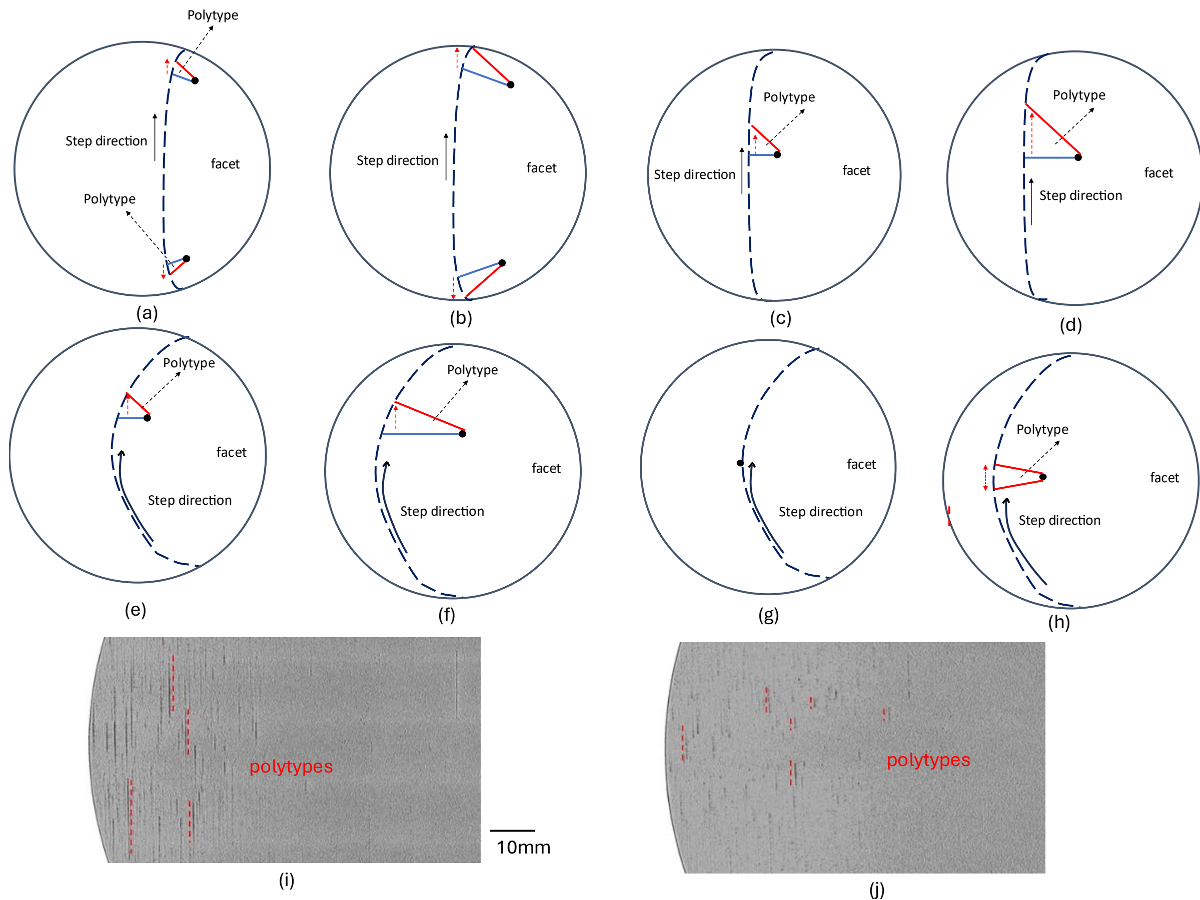

Fig. 5. Schematic of propagation and expansion of polytype with vertical step direction (a) and (b) near the edge; (c) and (d) near the center. Schematic of propagation and expansion of polytype with curved step direction (e) and (f) inner region of the wafer; (g) and (h) at the center of the curved step. HRXRD image of polytype of (i) wafer3 at early stage of the growth and (j) wafer7 at later stage of growth.

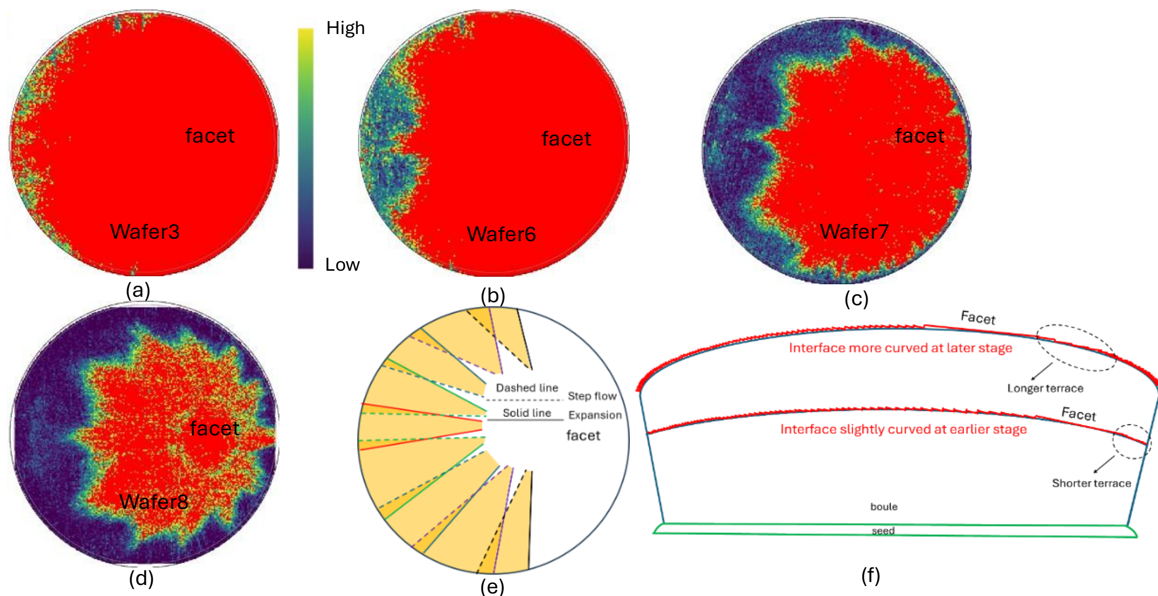

Fig. 6. TSDs/TMDs density map from HRXRD of (a) wafer3, (b) wafer6, (c) wafer7 and (d) wafer8, where red color means that TSDs/TMDs density is higher than manually set threshold value. (e) shows propagation and expansion of polytypes on the left side of the wafer resulting in gaps between that correspond to the shape of the TSDs/TMDs density map in (d). (f) shows change of width of terrace as growth proceeds. where the terraces on the left side of the facet is narrower initially, then become longer as the growth proceeds.

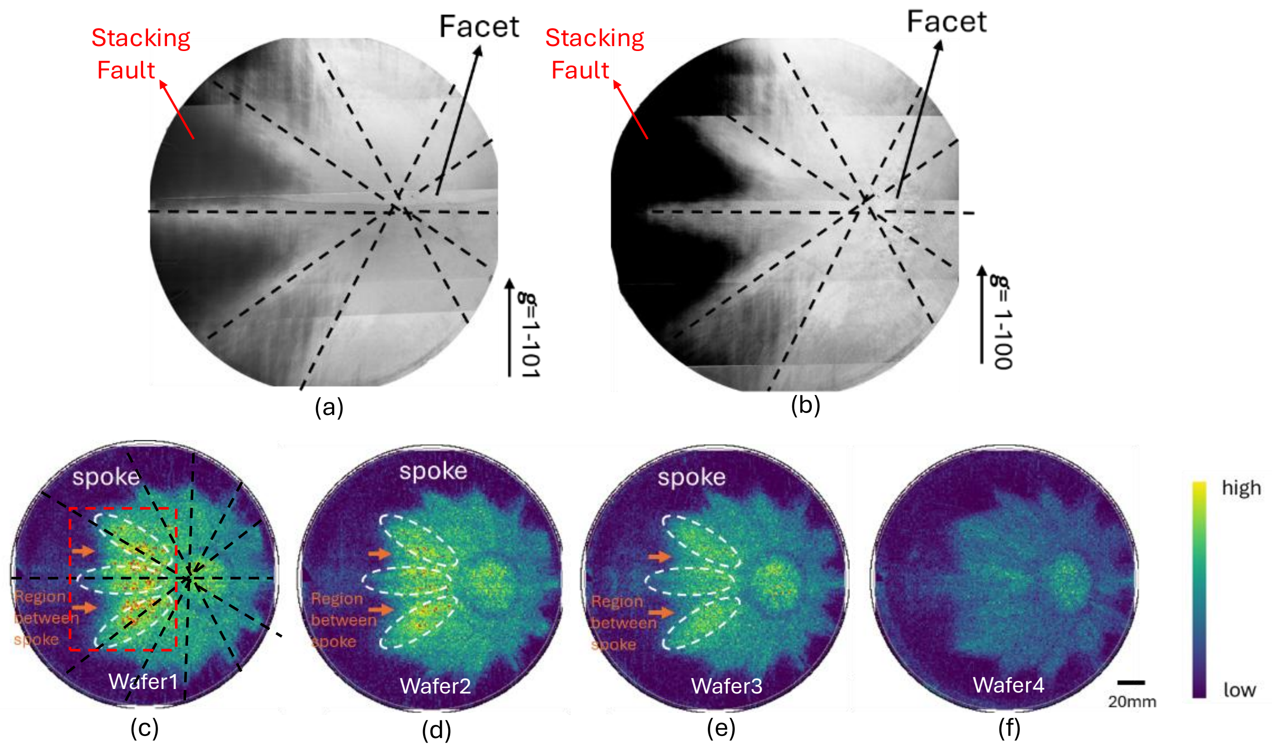

Fig. 7. SWBXT of wafer4 boule 2 in (a) 1-101 reflection and (b) 1-100 reflection, showing unique pattern of stacking faults where the spoke patterns are highlighted in dotted lines; (c) to (f): TSDs/TMDs density maps of wafers sliced from boule 2 at the position closer to the seed then further away from the seed.

Wafer4 of boule 2 was analyzed by synchrotron white beam X-ray topography (SWBXT) in 1-100 and 1-101 reflections. Mappings of TSDs/TMDs density for wafer1 to wafer4 sliced from boule 2 were conducted by HRXRD in 0008 reflection. As shown in Fig. 1, wafers sliced from boule 2 are from later stage of growth. Fig. 7(a) and 7(b) show the SWBXT in 1-100 and 1-101 reflections, where formation of stacking faults due to deflection of the TSDs/TMDs can be observed in the region between the spoke pattern which is highlighted by the dotted lines, where based on **g.b** analysis, majority of the stacking fault will be mixed type (Shockley+Frank), since 1-100 reflection shows stronger contrast of the faults [17]. Fig. 7(c) to 7(f) show density maps of TSDs/TMDs from the seed side (wafer1) to the dome side(wafer4), where higher density of TSDs/TMDs were observed near the facet region (Fig.7(c)) and the TSD/TMD density decreases as the wafer is closer to the dome side.

The pattern of wafer sliced from later stage of boule 2 show similarity to wafer8 of boule 1 (Fig. 6(d), indicating that deflections by polytypes exist in boule 2 as well. To further analyze the process, the TSDs/TMDs color maps are rescaled to see the difference on the spoke feature. Here, the spoke feature near the center of the wafer, highlighted by the red dotted box, will be specifically analyzed. Two areas with lower TSDs/TMDs density between the central spoke are highlighted by the white dashed line eclipse. Generally, TSDs/TMDs will have a faster growth rate than other parts of the crystal and form spiral steps during the growth [18], then when these steps merge, a growth island will be formed on the surface as shown in Fig. 8(a). When the growth proceeds, step bunching and polytypes will deflect TSDs/TMDs toward the step flow direction (Fig.8(b) and (c)). Since the density of TSDs/TMDs are lower on either side of the central spoke, as shown by the arrows of Fig.7(c), the growth rate along [000-1] will be slower in those regions, leading to ridge formation on the spoke positions, as shown in Fig.8(d). The ridge structure on the growth interface will be similar to star pattern observed from the facet [19]. Fig. 8(h) shows the top view of step structure of the ridge, where curved steps will form on the ridge (on the spoke position), while the valley will have normal steps conducive to forming a macrostep. Such step structure will suppress the formation of polytype on the ridge and the accumulated macrostep between the spoke can cause the deflection of TSDs/TMDs in

that region (Fig.8(e)), correlating with the decrease of TSDs/TMDs density between the spoke region in Fig. 7(d). Finally, as the growth interface becomes more convex, all the TSDs/TMDs will be deflected as shown in Fig. 8(f) and (g).

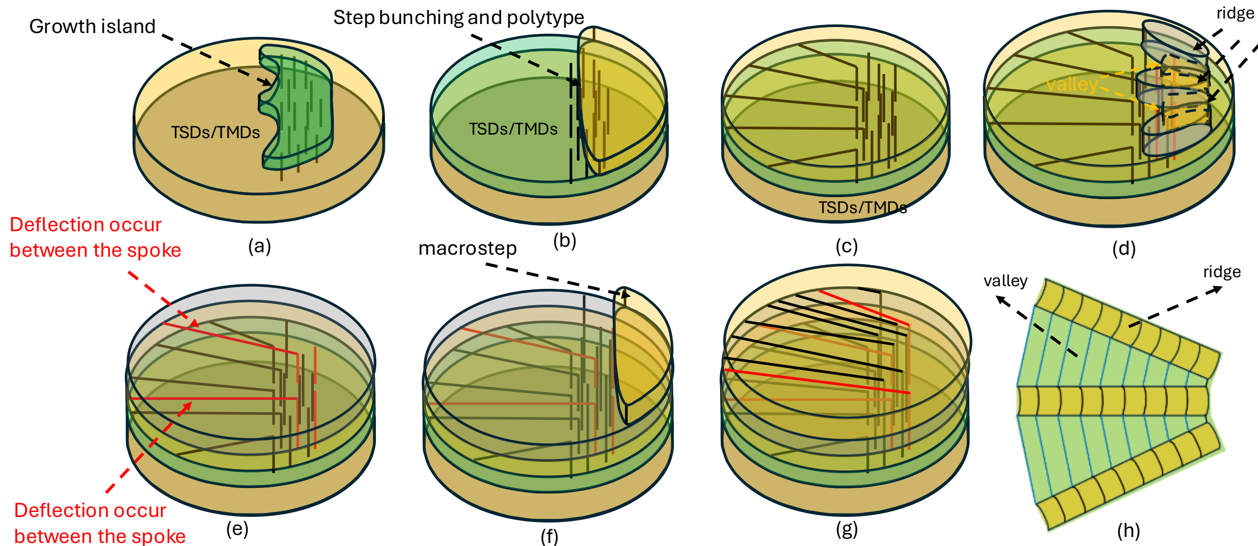

Fig. 8. 3D schematic of (a) growth island formed due to faster growth rate at the region with higher TSDs/TMDs density, (b) and (c) deflection of TSDs/TMDs by step bunching and polytype, (d) ridge structure formation due to difference in TSDs/TMDs density, (e) deflection process between the spoke region, (f) and (g) defection of TSDs/TMDs by macrostep; (h) step structure on the ridge and valley.

Summary

Synchrotron monochromatic beam X-ray topography, synchrotron white beam X-ray topography and high-resolution X-ray topography were used to characterize series of wafers sliced from two PVT-grown 4H-SiC boules grown under similar conditions. Spoke pattern on TSDs/TMDs density map can be observed from wafer sliced from later stage of growth of both boules. Deflections of TSDs/TMDs by 2D nucleated thin polytype layers due to relatively fast growth rate have been observed, since Burgers vector of TSDs/TMDs in 4H structure is not compatible in polytype. The polytypes will propagate and expand, where one of the edges will follow the step flow direction and the other edge will expand along [1-100] and [-1100] directions. At the early stage of growth, the polytype will expand quickly due to vertical step structure, while it will slow down when the step structures become curved at the later stage of growth. The difference in direction between the propagation edge and the expansion edge facilitates the formation of the spoke pattern. Such pattern will give rise to faster growth rate along [000-1], leading to formation of ridge on the growth interface. The ridge structure will suppress the formation of polytype on the ridge and also accumulate macrosteps between the spokes that subsequently cause the deflection of TSDs/TMDs and formation of stacking faults. Processing parameters such as growth rate should be optimized to avoid formation of the polytypes and the deflections of TSDs/TMDs.

Acknowledgement

Work supported by Onsemi. This research used resources of the National Synchrotron Light Source II, a U.S. Department of Energy (DOE) Office of Science User Facility operated for the DOE Office of Science by Brookhaven National Laboratory under Contract No. DE-SC0012704. This research used resources of the Advanced Photon Source (Beamline 1-BM), a U.S. Department of Energy (DOE) Office of Science User Facility operated for the DOE Office of Science by Argonne National Laboratory under Contract No. DE-AC02-06CH11357. The Joint Photon Sciences Institute at SBU provided partial support for travel and subsistence for access to Advanced Photon Source.

References

[1] A.A. Lebedev and V.E. Chelnokov, Semiconductors 33, 999–1001 (1999).

[2] Y. M. Tairov and V.F. Tsvetkov, Journal of Crystal Growth 43(2), 209-212 (1978)

[3] P. Bergmanet al, Mater. Sci. Forum 353-356, 299-302 (2001)

[4] P. G.Neudeck et al, Solid-State Electronics 42(12), 2157-2164 (1998).

[5] M. Dudley; X. R. Huang; W. Huang; A. Powell; S. Wang; P. Neudeck; M. Skowronski, Appl. Phys. Lett. 75, 784–786 (1999)

[6] Tsunenobu, K.; Cooper, J. A., Fundamentals of Silicon Carbide Technology: Growth, Characterization, Devices and Applications; Wiley, 2014.

[7] J. Li, G. Yang, X. Liu, H. Luo, L. Xu, Y. Zhang, C. Cui, X. Pi, D. Yang and R. Wang, J. Phys. D: Appl. Phys. 55 463001(2022)

[8] Q. Y. Cheng, H. Y. Peng, Z. Y. Chen, S. Hu, Y. Liu, B. Raghothamachar, M. Dudley, Defect and Diffusion Forum, 426, 57-64 (2023)

[9] M. Dudley, H.H. Wang, F.Z. Wu, S.Y. Byrapa, B. Raghothamachar, G. Choi, E. Sanchez, D.M. Hansen, R. Drachev, S.G. Mueller, Mater. Sci. Forum 679, 269-272(2011)

[10] Y. Yang, J. Guo, O. Goue, B. Raghothamachar, M. Dudley, G. Chung, E. Sanchez, J. Quast, I. Manning, D. Hansen, J. Electron. Mater. 45, 2066-2070 (2016)

[11] J. P. Bergman, H. Lendenmann, P. A. Nilsson, U. Lindefelt and P. Skytt: Mat. Sci. Forum, 353-356 299(2001)

[12] A. Galeckas, J. Linnros, P. Pirouz, Appl. Phys. Lett. 81 883. (2002)

[13] A. Agarwal, H. Fatima, S. Haney, S. H. Ryu, IEEE Elec. Dev. Lett. 28, 587. (2007)

[14] N.A. Mahadik, M. Dudley, B. Raghothamachar, Z. Chen, R.E. Stahlbush, M. Hinojosa, A. Lelis, W. Sung, Materials & Design, 248 113435 (2024)

[15] H. Peng, T. Ailihumaer, Y. Liu, B. Raghothamachar, X. Huang, L. Assoufid, M. Dudley. Journal of Applied Crystallography 54, 1225-1233 (2021)

[16] T. Ailihumaer, H. Peng, Y. Liu, B. Raghothamachar, M. Dudley, G. Chung, I. Manning and E. Sanchez, J. Electron. Mater. 50, 3258–3265 (2021)

[17] M. Dudley, F. Wu; H. Wang, S. Byrappa, B. Raghothamachar, G. Choi, S. Sun, E. K. Sanchez, D. Hansen, R. Drachev, S. G. Mueller and M. J. Loboda, Appl. Phys. Lett. 98, 232110 (2011)

[18] WK Burton, N Cabrera, FC Frank, Philosophical Transactions of the Royal Society of London. Series A, Mathematical and Physical Sciences 243.866, 299-358 (1951).

[19] M. Sonoda, T. Nakano, K. Shioura, N. Shinagawa, N. Ohtani, Journal of Crystal Growth, 499 24-29 (2018).